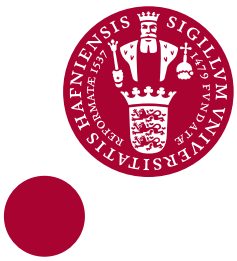

Two and three dimensional redox heterogeneity of rat liver. Effects of anoxia and alcohol on the lobular redox pattern.

Quistorff, Bjørn; Chance, Britton; Takeda, Heroshi

Published in:
Frontiers of Biological Energetics

Publication date:
1978

Document version
Publisher's PDF, also known as Version of record

FRONTIERS OF BIOLOGICAL ENERGETICS, VOLUME 2

TWO- AND THREE DIMENSIONAL REDOX HETEROGENEITY OF RAT LIVER. EFFECTS OF ANOXIA AND ALCOHOL ON THE LOBULAR REDOX PATTERN.

Bjørn Quistorff

Department of Biochemistry A
University of Copenhagen
Denmark

Britton Chance
Heroshi Takeda

Johnson Research Foundation
University of Pennsylvania
Philadelphia, PA

I. ABSTRACT

3-D Recordings of redox state has been carried out in freeze-clamped samples from perfused rat liver at a resolution of 8000 single point measurements per mg. of tissue. The redox state is measured as the ratio between the fluorescence intensities of oxidized flavoprotein (FP) and reduced pyridine nucleotide (PN). A periportal-periveneous redox gradient is observed in the normoxic rat liver. The steepness of this gradient is enhenced by acute alcohol treatment while complete anoxia eliminates the gradient. 3-D metabolic structures, interpretable with respect to liver morphology, may be recognized in a tissue volume reconstructed from scanning data in controls as well as in alcohol treated livers.

II. INTRODUCTION

Most biochemical work on mammalian liver has so far been based on the assumption of a metabolically homogeneous population of hepatocytes. However, histochemical studies clearly show enzyme activity differences within the microcirculatory unit of the normal liver. Furthermore, a number of pathological conditions show that different hepatocyte populations are highly specific in their response to toxic agents. For a recent review, see Rappaport (1). Based on such information on cell heterogeneity, a concept of functional metabolic zonation of the liver acinus has developed which proposes

ISBN 0-12-225402-3

that oxidative processes mainly occur in the periportal area of the acinus while, biosynthetic processes are located in the perifery of the acinus, i.e. are perivenous. The zonation is not thought to be a static organization of metabolism, but rather a functional separation dictated by the actual substrate and product gradients along the sinusoid. For a recent review see Jungermann and Sasse (2).

This report presents data supporting the concept of metabolic heterogeneity in the liver acinus. Experiments have been carried out in order to map 2- and 3-dimensional redox gradients in the normoxic, anoxic and alcohol treated perfused rat liver. A recently developed low temperature redox ratio scanning instrument has been employed. The instrument allows recording redox states in three dimensions, with a resolution of less than $3 \times 10^{-4} mm^3$, corresponding to about 20 hepatocytes. Preliminary accounts of these data have been given (3,4).

III. MATERIALS AND METHODS

1. Liver Perfusion. Well fed, male wistar rats, weighing about 300 g were used. Anaesthesia was produced with pentobarbital I.P., 50 mg/kg and a flow through perfusion of the liver was set up according to the procedure described in (5). The perfusion media was Krebs-Henseleit bicarbonate buffer equilibrated with O_2/CO_2 : 95/5 at 37°C. In all experiments the perfusion period was 30 min., after which the liver was freeze clamped (see below). Ethanol was added to the perfusion medium after 15 min. of perfusion, to a final concentration of 6.2 mM. Anoxia was introduced by substituting nitrogen for oxygen in addition, prior to freeze clamping the liver was left unperfused on ice for 10 min. In all experiments the liver was covered with oxygen-impermeable Saran Wrap. ®

2. Freeze Clamping. The freeze clamping procedure serves a dual purpose: to stop metabolic processes, and to fix the frozen sample mechanically to the sample holder. The instrument used for the process is shown in Figure 1. The anterior, medial lobe of the liver was held between the pre-cooled branches of the freeze clamping tongs with the anterior surface upwards. Upon clamping, the liver adapts to the shape of the chamber formed between the two blocks of the freeze clamping tongs, B_1 and B_2, while excess tissue is squeezed out (see Fig. 1). The clamping is performed rather gently to minimize distortion of the liver morphology (6). In the frozen

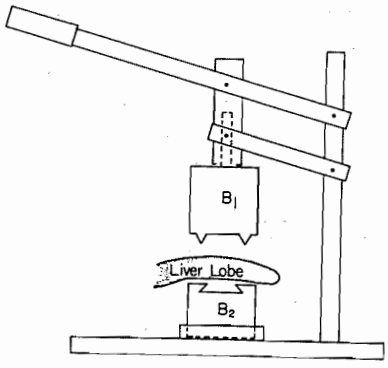

BQ 152

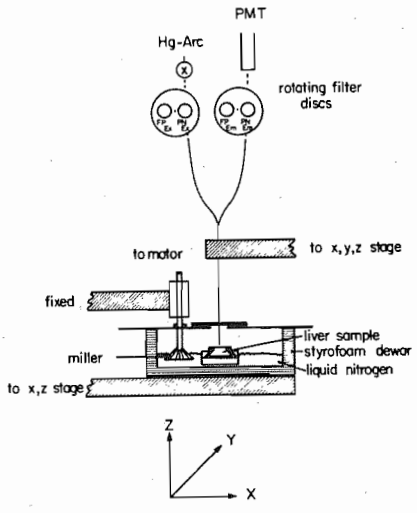

BQ 149

FIGURE 1. Freeze clamping instrument. The cylindrical shape aluminium blocks, B_1 and B_2 are pre-cooled in liquid nitrogen and then mounted in the tongs 20 - 30 sec. before clamping.

FIGURE 2. Low temperature scanning instrument. During scanning the light guide are moved in the x-y plane in a vertical position while the sample is fixed. For cutting, the sample is moved down along the z-axis until the difference in z-level between sample surface and cutter plane equals the desired thickness of the cut. The cut is now performed moving the sample along the x-axis underneath the cutter.

state the sample is firmly attached to the sample block with the original surface of the liver lobe oriented parallel to the block, B_1.

3. Scanning. A simpler version of the scanning instrument, as applied to brain tissue, has been described before (7). Only a brief description of the present instrument will be given here (8), but a detailed account will appear later. The fluorescence intensities of oxidized flavoprotein (FP) and reduced pyridine nucleotide (PN) are measured at single points by surface fluorescence at $77^{\circ}K$. The ratio FP/PN is taken as a measure of the tissue redox state (7,9). The scanning instrument is shown schematically in Figure 2. A micro-light-guide with a fiber diameter of 50μ provides the optical coupling between the dual disc fluorometer

the sample surface. The tip of the light guide is kept at a distance of 30μ from the surface of the sample. At this distance the optical signal is picked up from a spot of a diameter of about 60μ. Tissue below a depth of 50 - 100μ does not contribute significantly to the total signal. PN fluorescence was excited at 366 nm and measured at 450 nm. The corresponding wavelengths for FP were 436 and 560 nm. The scanning procedure is as follows: the sample is mounted in the chamber partly submerged in liquid nitrogen (see Fig. 2). Before initiating a scan, a cut to remove 50 - 100μ of tissue is made with a low temperature cutter built together with the scanner in order to create a smooth surface exactly parallel to the scanning plane (6). The light-guide is then adjusted to the correct height above the tissue surface and the scan is performed by moving the light-guide across the surface in a Raster-Pattern in steps of 50μ while FP and PN signals are recorded at each point and stored with the appropriate x-y coordinates in a PDP 11/10 mini computer. When a scan is completed, a tissue layer of 50μ is cut off as described above, and the scanning is resumed over an area which is exactly below the first scan. A suitable number of consecutive scans are collected. In the experiments presented here, 8 - 13 scans were collected. The tissue volume covered in a 10 section scan is typically 4 x 4 x 0.6 mm, with a total of 65610 single point measurements of FP and PN.

4. Data Display. The scanning data are available from the computer in several forms. For quantitative data evaluation we have used the 2-D matrix and a histogram display of all FP/PN measurements from each single scan. Gray-scale television displays of the 2-D FP/PN matrix of the single scan have served for the qualitative evaluation of the redox patterns. The 2-D matrix represents a two dimensionally ordered printout of the digitized fluoresence intensities (FP/PN = CR). These numbers may be translated to a gray-scale (high CR becomes white, low CR becomes black) and displayed as a 2-D metabolic image of the tissue area which was scanned. The virtue of the histogram display is the inherent high sensitivity for detection of small fractions of points of a scan which differs significantly but which are easily overlooked on the 2-D matrix.

IV. RESULTS

1. Reliability of the freeze-trapping procedure. An important consideration using the approach described here to

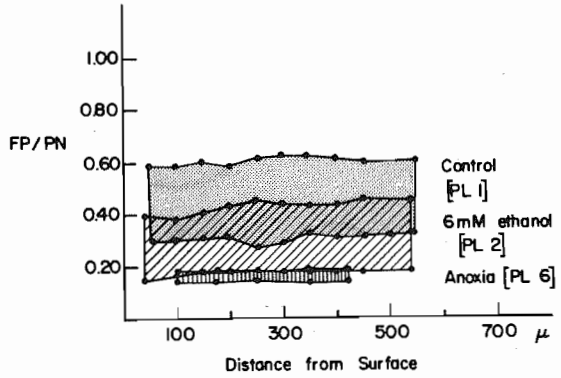

BO 150

FIGURE 3. Effect of ethanol and anoxia on the redox range in serial scans. The range is obtained from the FP/PN ratio histograms of the individual scans defining the range as the 5% and 95% cut off lines. The distances shown on the x-axis represents the depth in which the scan was performed.

obtain 3-D metabolic information is whether the freeze clamping actually traps the metabolic state fast enough in all parts of the tissue block used for scanning. Figure 3 suggests that this is the case by showing essentially no change in redox range with increasing scanning depth. Furthermore, in experiments with uncoupler (not shown) where oxygen demands are maximal (average CR increased to 180% of control), the redox ratio range remains unchanged to a scanning depth of 1100μ. This figure corresponds well with what is observed as the depth to which metabolic state is trapped by freeze clamping in brain (7) and muscle (10).

2. Effects of anoxia and alcohol. Figure 3 shows the effect on redox range (defined in figure legend) of consecutive scans by anoxia and alcohol. Complete anoxia decreases the average redox ratio to about 25% of the control. In addition a very narrow redox range is observed suggesting that the liver morphology per se and the inhomogeneous enzyme distribution across the acinus will not contribute significantly to the redox pattern observed under other experimental conditions. Alcohol descreases the average CR value by approximately a factor of 2 corresponding well with the increase found for the β-hydroxybutyrate-acetoacetate couple, although rather smaller than for the lactate/pyruvate couple as determined by chemical analysis of freeze clamped samples from perfused liver (11). There is a 40 - 50% overlap between the

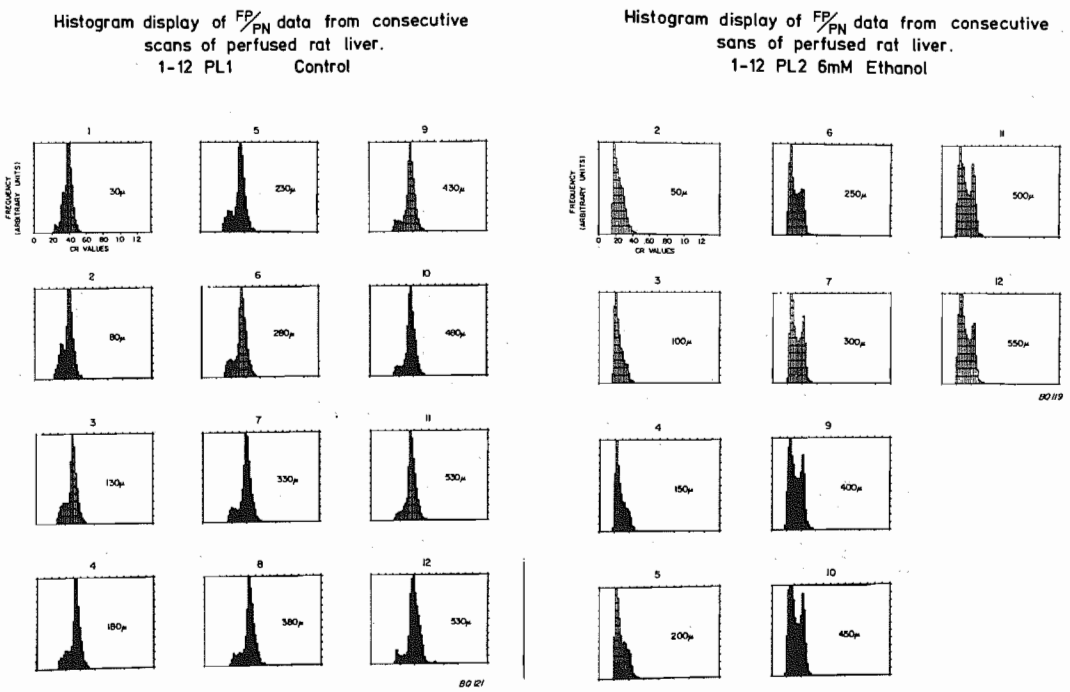

FIGURE 4. Effect of ethanol on the redox ratio histogram of serial scans. Left panel represents a control liver and right panel an ethanol treated liver (6.2 mM). The y-axis is not identical in all scans. However, the total sum of bar heights is 3600 in all histograms, i.e. the total number of points per scan. The depth in which the individual scan was performed is indicated on each histogram.

redox range of control and alcohol livers but also a small overlap between anoxia and alcohol. This seems to indicate that some regions are maximally reduced during alcohol oxidation while others are not affected beyond the control redox range.

The effects of alcohol are further elucidated in Figure 4 which gives the histogram display of a series of scans of a control as well as an alcohol treated liver (see Materials and Methods). The control histogram appears roughly bell-shaped with no significant difference between individual scans. Upon addition of alcohol, however, marked changes may be observed: First - a very steep rise of the low CR part of the histogram is seen through all scans underlining the points made above that a substantial fraction of cells become maximally reduced by alcohol, otherwise, one would have expected the histogram to tail off towards reduction. Second - there is an overall shift of 50% of the histogram towards reduced levels. Third - at a certain depth, in this experiment about 300 μ, the histogram assumes a bimodal shape which is present in all following sections. It should be noted, however, that in some experiments with alcohol, we do not observe bimodal histograms, although the two other characteristics mentioned above are still present. The significance of this is not understood at present. The fact that bimodal histograms are not observed in the first few scans of alcohol treated livers is ascribed to the special morphology of the liver: the liver aceni close to the liver surface are roughly spheric shaped, approxiately 600 μ in diameter (1). Thus, assuming concentric distribution of redox heterogeneity in the acinus, one would not expect to find major heterogeneity in sections at a level much above half the diameter of the outermost acini as these sections will cut most sinusoids at about the same periportal-periveneous level. In deeper sections, however, the sinusoids will be cut at all levels and the histogram will display the metabolic heterogeneity present in the aceni.

3. Resolving the redox pattern. Figure 5 shows a television display of scans from a control and an alcohol treated liver. The FP/PN ratio is displayed on a grey-scale with white and black representing oxidized and reduced, respectively (for details, see Figure legend). The control scan, Figure 5A, may be described as regularly scattered black dots on a white-grey background. The black dots are mostly of circular shape, 300-600 μ in diameter with a border zone of 100-200 μ. We interpret this pattern in terms of the black dots being reduced periveneous zones (around a terminal hepatic vein). Conversely the white-grey background represents a confluence of relatively oxidized periportal spaces. The CR range for the

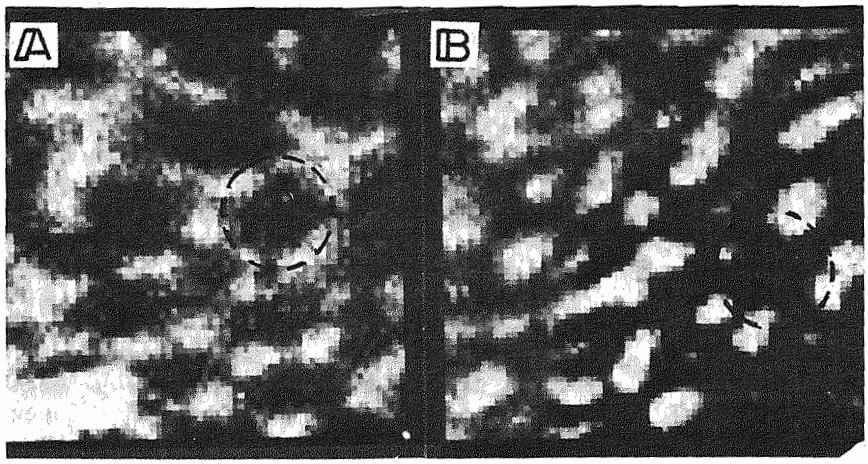

FIGURE 5. Television gray-scale display of scans of liver. The scan was performed in a depth of 350μ below the surface of the freeze clamped sample. The scan area was 3.55 x 3.55 mm and step size was 50μ, i.e. 5041 points. A is control, B is with 6.2 mM ethanol in the perfusion medium. FP/PN ratio is displayed - white represents oxidized (high FP/PN) and black reduced (low FP/PN). The gray-scale has been chosen slighlty different for the two pictures in order to resolve the pattern better.

periveneous space is 0.35 - 0.42 and 0.45 - 0.50 for the periportal. Moving on to the ethanol perfused liver, Figure 5B, one finds similar oxidized and reduced zones, although the pattern looks quite different from the control. Now the black periveneous spaces are confluent, isolating white relatively oxidized periportal spaces. In other words, the effect of alcohol on the redox pattern is an increase of the reduced periveneous area at the expense of the periportal area with a much steeper transition in between. In most locations the transitions occurs within the linear resolution of the scanning instrument, i.e. 50μ. The CR range for the periveneous area is 0.18 - o.28 and for the periportal 0.36 - 0.41.

It should be noted that in the alcohol liver, Figure 5B, the shape of the periveneous area (black) is very similar to the so called star-fish figure found histologically in the liver with various pathological conditions (1). Being aware of this pattern, one may also recognize it in the control scan. A classical liver lobule is encircled on both scans.

Figure 6 shows a 3-D representation of a 10 section scan of

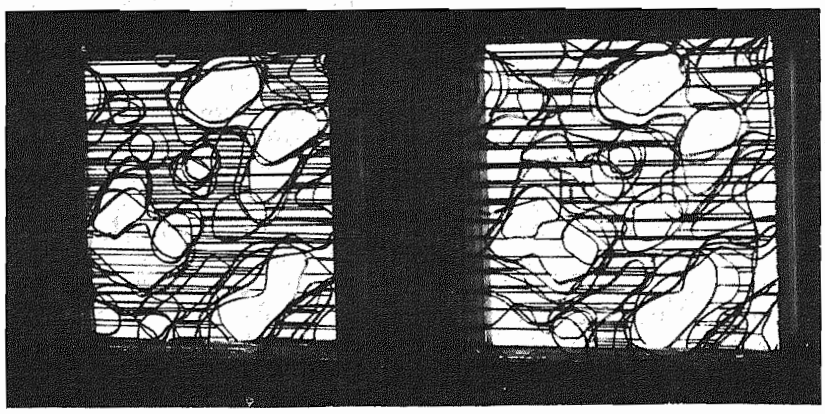

FIGURE 6. 3-D redox model of ethanol treated liver. The model was constructed by tracing the FP/PN border zone contour between periportal and periveneous spaces from 10 consecutive scans of an alcohol treated liver (6.2 mM). The tracing was done on Lucite plates from the 2-D FP/PN matrix. The plates were then assembled and photographed. A pseudo-stereoscopic effect is obtained by separating the scan in two stacks, odd numbers are displayed left and even numbers right. The tissue volume covered by the model is $1.75 \times 1.75 \times 0.55$ mm. Scanning step size was 50 μ.

an alcohol treated liver. The model was composed with only two grey levels since, as noted in Figure 5, there is a quite well defined border-zone between oxidized and reduced in the alcohol treated liver. The cross-hatched black is reduced and white is oxidized. A number of cylindrical or ellipsoidal relatively oxidized bodies oriented roughly perpendicular to the surface may be recognized, indicating that the pattern found in the 2-D scans is actually part of a 3-D redox structure. In analogy with what was argued above for the relation between the 2-D redox pattern and liver anatomy, these relatively oxidized bodies in Figure 6 are tentatively identified with the central parts of simple acini.

V. DISCUSSION

The 2- and 3-D scanning data presented clearly show the existence of a spatially organized redox structure of the perfused rat liver which may be characteristically affected by

various redox pertubations. The metabolic structure is tentatively identified in terms of liver anatomy as relatively oxidized zones around the terminal portal veins and reduced zones around the terminal hepatic veins; thus, defining a longitudinal sinusoidal redox gradient. Matschinsky et al. (12) recently measured regional concentration of oxidized and reduced pyridine nucleotide in the liver but found essentially no change in $NAD_{total}/NADH_{total}$ between periportal and periveneous regions. This apparent discrepance is probably in part explained by the fact that the two techniques measure different parameters: the redox ratio will mainly reflect the mitochondrial redox state (7,9) while the chemical analysis integrates all cell compartments and measures free as well as bound pyridine nuclotide. Also, since the scanning technique reveals considerable variation in shape and magnitude of the sinusoidal redox gradient within the same liver, the relative small number of acini probed with the micro dissection technique might bias the results.

It is not obvious what causes the redox gradient observed along the sinusoid. However, if the redox gradient in the normoxic liver primarily reflects an oxygen gradient, the effect of alcohol may be explained simply by the small but significant increase in oxygen consumption found in livers from fed rats (13). This will cause an intolerable decrease in oxygen tension in the distal end of the sinusoid and consequently hypoxia in periveneous cells (14). However, it is difficult to understand how oxygen could be limited in any part of the normoxic perfused liver since the effluent P_{O_2} is at least two orders of magnitude higher than the apparent K_m for oxygen for isolated mitochondria and since diffusion distances seem to be smaller than a cell diameter (15). It should be noted though, that evidence for very steep oxygen gradients in the perfused liver has been published recently (16).

At present we therefore interpret the effect of alcohol in terms of the existence of two populations of hepatocytes in the liver which reacts qualitatively and/or quantitatively different to alcohol. Regional differences in alcoholdehydrogenase activity might play a role. However, the activity differences reported are small (17) and furthermore, alcohol dehydrogenase activity is unlikely to be rate-limiting in alcohol oxidation under the present experimental conditions (18).

ACKNOWLEDGEMENTS

The authors wish to thank Mrs. Elisabeth Joice, Dr.Charley Noback, and Dr.John Haselgrove for valuable discussion and help. This research was supported by NINDS NS10939.

REFERENCES

1. Rappaport, A.M. (1976). Beitr.Path. Bd.157, 215-243.
2. Jungermann, K., and Sasse, D. (in press). In "Micro-environments and Cellular Compartmentation" (P.A. Srere and R.W.Estabrook, eds.). Academic Press, New York.
3. Quistorff, B., and Chance, B. (1977). Hoppe-Seyler's Z. Physiol. Chem. 358:1261.
4. Quistorff, B. and Chance, B. (1977). Federation Proc. 36: 1358.
5. Scholz, R., Hansen, W., and Thurman, R.G. (1973). Eur. J. Biochem. 38:64-72.
6. Quistorff, B., and Chance, B. (in preparation). Anal. Biochem.
7. Quistorff, B., and Chance, B. (1976). In "Oxygen and Physiological Function" (F.F.Jóbsis, ed.), p.100. Professional Information Library, Dallas, Texas.
8. Haselgrove, J., Barlow, C., Chance, B., Joyce, E., Kanamuller, H., and Bruckner, M. (this volume) "Frontiers of Biological Energetics". Academic Press, New York.
9. Chance, B., Oshino, R., Itshak, F., and Nakase, Y. (in preparation).Anal. Biochem.
10. Kretzschmer, C.C., Wilkie, D.R., and Woledge, R.C. (1971). J.Physiol. 218:163-193.
11. Bücher, T., and Sies, H. (1976). In "Use of Isolated Liver Cells and Kidney Tubules in Metabolic Studies". J.M. Tager, H.D.Solling, and J.R.Williamson, eds). North Holland Publishing Co., Amsterdam.
12. Matschinsky, F.M., Hintz, F.M., Reichlmeir, C.S., Quistorff, B., and Chance, B. (in press). In "Micro-environments and Cellular Compartmentation" (P.A. Srere, and R.W.Estabrook, eds.). Academic Press, New York.
13. Thurman, R.G., and Scholz, R. (1977). Eur.J.Biockem. 75:13-21.
14. Israel, Y., Kalant, H., Khanna, J.M., and Orrego, H. (1977). In "Alcohol Intoxication and Withdrawl-III". (M.M. Gross, ed.), p.343. Plenum Press, New York.
15. Chance, B., Schnener, B., and Schindler, F. (1964). In "Oxygen in Animal Organisms" (F.Dickens, and E.Niel, eds.), p.367. Pergamon Press, London.
16. Sies, H. (1977). Hoppe-Seyler's Z.Physiol.Chem. 358:1021-1032.
17. Greenberger, N.J., Cohen, R.B., and Isselbacker, K.J. (1965). Lab.Invest. 14:264.
18. Lundquist, F., Damgaard, S.E., and Sestoft, L. (1974). In "Alcohol and Aldehyde Metabolizing Systems". (R.G. Thurman, et al., eds.), p.405. Academic Press, New York.